

A Mass And Time-Of-Flight Spectroscopy Study Of The Formation of Clusters In Free-Jet Expansions of Normal-D₂

Y. Ekinçi,* E.L. Knuth[†] and J.P. Toennies

Max-Planck-Institut für Dynamik und Selbstorganisation, Bunsenstr. 10, 37073 Göttingen, Germany

**Current address: Paul Scherrer Institute, Laboratory for Micro and Nanotechnology, CH-5232, Villigen PSI, Switzerland*

[†]Permanent address: Department of Chemical and Biomolecular Engineering, University of California at Los Angeles, Los Angeles, California 90095

Abstract. The mass spectra in the range $2(\text{D}^+)$ - $38(\text{D}_{19}^+)$ amu of clusters formed in a supersonic free-jet expansion of normal D₂ are investigated as functions of source temperature in the range 95-220 K and of source pressure in the range 10-120 bar. Time-of-flight (TOF) distributions are measured for some of the small ion fragments. For large clusters ($n > 200$) the intensities of the odd-numbered ion fragments exhibit magic numbers at D_9^+ and D_{15}^+ in accordance with previous experiments and calculations. The even-numbered ion fragments have much smaller intensities and exhibit new magic numbers at D_{10}^+ and D_{14}^+ . For source conditions such that large clusters are formed, the intensities of the various ion fragments are observed to saturate beyond a certain source pressure. At lower source pressures, where only small clusters are formed, the terminal mole fractions of the neutral dimers are analyzed taking into account both the thermodynamics and the kinetics of the expansion. At higher source pressures and lower temperatures, where larger clusters are formed, the sizes of the neutral clusters are estimated using scaling laws and are found to be consistent with the mass spectra and measured TOF distributions. The use of a variety of techniques facilitated obtaining reliable conclusions about the neutral-cluster sizes for the present free-jet expansion conditions.

Keywords: Cluster formation, cluster sizes

PACS: 39.10.+j, 36.40.-c

INTRODUCTION

Molecular beams formed from free-jet expansions are characterized by high intensities, well-defined energies and low internal temperatures. This makes them an important research tool. Under special conditions, weakly bound van der Waals complexes and clusters, not otherwise easily accessible, are formed. Clustering and condensation have been and still are objects of intensive research activity with motivations such as to study the kinetics of cluster formation and to explore the evolution of physical properties from molecular to bulk sizes.

The first observation of cluster formation was by Becker et al. [1] in 1956. They observed unexpected changes of the intensities, velocities and speed ratios of H₂, N₂ and Ar beams with decreasing stagnation temperature and increasing stagnation pressure, and attributed their observations to condensation. Subsequent studies by other groups have examined the formation of small clusters of H₂ [2-7] and large clusters of H₂ [8-16] and D₂ [17, 18]. Several criteria for correlating the onset of condensation have been proposed [19,20]; also several nucleation models which provide empirical estimates of terminal cluster concentrations for specific cases [21-26]. Hagena and Obert developed empirical scaling laws for predicting the onset of clustering and for correlating cluster size [25, 26]. Knuth used a relatively simple sudden-freeze model to extract recombination coefficients from measured terminal dimer mole fractions in free jets of rare gases [27]. By identifying dimensionless parameters generated when one writes the equation describing nucleation in dimensionless form, he extended Hagena and Obert's scaling parameters and found a good correlation of cluster size with scaling parameter for the rare gases [28].

In the present investigation, small and large neutral D_2 clusters formed in free-jet expansions are studied over a wide range of source temperature and pressure. The mass spectra and TOF distributions, analyzed with the help of size correlations [28] and new results on fragmentation [29], provide reliable estimates of neutral cluster size.

APPARATUS AND EXPERIMENTAL CONDITIONS

The molecular-beam apparatus, described in detail elsewhere [30], was designed for surface-scattering experiments, but allows investigations of free-jet beams by moving the target out of the beam path and rotating the detector into the beam direction. The beam is generated by expanding high-purity normal- D_2 from a high pressure into a vacuum through a small orifice; it is detected, after travelling about 3 meters and passing through seven differential pumping stages, by an electron-bombardment ionizer followed by a magnetic mass spectrometer. The beam source consisted of a 10-mm-diameter, 5-cm-long stainless-steel tube cooled by liquid nitrogen. The desired temperature, T_0 , is achieved by a heating coil at the orifice end and monitored by a Pt-100 thermistor located between the heating coil and the orifice. The temperature is regulated by a controller within the range 95-400 K to within 0.1 K. The source pressure, P_0 , is measured with a precision ($\pm 1\%$) Bourdon gauge. The beam orifice is a circular pinhole in a Platinum plate and has a nominal diameter of 10 μm and a length of about 5 μm . The commercial nickel skimmer has a length of 25 mm with a 400- μm -diameter opening. The total included internal and external angles of the conical skimmer are 25° and 30° respectively. The nozzle-to-skimmer distance is fixed at 7.5 mm. The base pressure of the source chamber is 1×10^{-7} mbar and rises to less than 10^{-3} mbar with the beam on.

The home-made detector incorporates an electron-bombardment ionizer, extractor and focusing optics, a 90° magnetic mass spectrometer, and a channeltron multiplier for ion detection and amplification. Since the counting electronics is only able to handle signals of less than 10^6 cts/sec, larger signals had to be attenuated by lowering the emission current of the detector and/or degrading the ion-focusing optics.

The velocity distributions are determined using the TOF method. The beam is chopped by a 0.1-mm-thick, 138-mm-diameter metal disk with two diametrically positioned 2-mm-wide slits.

EXPERIMENTAL RESULTS

D_2^+ is found to be the largest peak in all the mass spectra measured here -- consistent with earlier measurements on H_2 and D_2 clusters [2, 18]. Its magnitude is nearly constant and independent of both the source temperature and the source pressure. See, e.g., the dependence on P_0 for $T_0 = 220$ K displayed in Fig. 1. This remarkable behavior suggests strongly that the D_2^+ signal is due largely to free unclustered D_2 molecules in the beam. Hence the nearly invariant D_2^+ signal indicates that the D_2 density in the free jet does not scale with source pressure. Apparently the increase in monomer flux with increase in source pressure is nearly cancelled by the increase in monomer consumption due to cluster formation. The heavier fragment peaks are distributed over the odd-numbered ion peaks and have intensities lying between 0.05% and 3% of the D_2^+ signal. Even-numbered ion peaks with smaller intensities by one to two orders of magnitude are seen clearly up to D_{14}^+ .

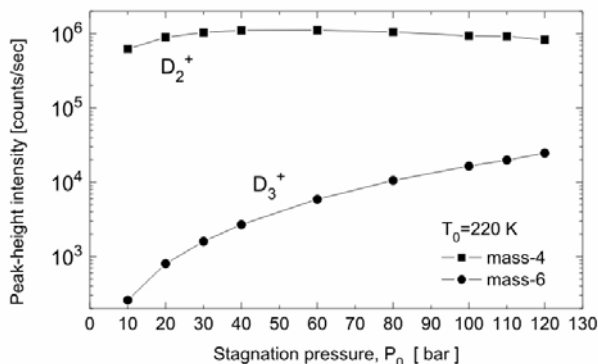


FIGURE 1. The intensities of the ion fragments D_2^+ and D_3^+ for $T_0 = 220$ K as functions of P_0 . Source-orifice diameter is 10 μm .

The area under each peak was used to analyze quantitatively the mass spectra. An examination of the dependence of the ratio D^+/D_2^+ on T_0 suggests that the D^+ ions originate not only from the D_2 molecules and small clusters but also to a significant extent from large clusters.

The peak-area intensities of the D_9^+ and D_{15}^+ ions are found to stand out above those for the other odd-numbered ions. These “magic numbers” have been noted in previous studies and are attributed to their special geometries. Although the resolution is not sufficient to resolve completely the peaks at large masses, the even-numbered peaks at D_{10}^+ and D_{14}^+ appear also to be magic numbers. Similar magic numbers for even-numbered ions appear to have been detected some time ago in a positive-ion trap filled with H_2 gas [31].

Complementary information on cluster formation in these free-jet expansions is gained from TOF measurements. In these measurements, the focus was on the dimerization regime, in which the source pressure is sufficiently low so that the beam consists mainly of monomers and dimers and only the corresponding small ions are observed. Typical TOF spectra of D_2^+ and D_3^+ cluster ions at a stagnation temperature of $T_0 = 220$ K and three different stagnation pressures under “dimerization” conditions are shown in Fig. 2. The source-pressure dependencies of the speed ratios and velocities extracted from TOF spectra at $T_0 = 220$ K are shown in Fig. 3. The observed increase of the velocity with increasing source pressure indicates a more extensive conversion of the source-gas enthalpy, including the energy of the rotational degrees of freedom, into the terminal beam velocity. In Fig. 2, the D_2^+ and D_3^+ cluster ions have identical velocities but different speed ratios. If the monomers and dimers have nearly the same velocities and random-translational temperatures, then the ratio of speed ratios should be the square root of 2. The observed nearly constant square-root-of-2 ratio of speed ratios confirms that the random-translational temperatures of the monomers and dimers are nearly equal.

DIMER FORMATION

Here the formation of dimers in the dimerization region is examined in detail. Recent extensive matter-wave diffraction measurements of small neutral H_2 clusters in our laboratory [29] provide the first reliable measurements of the ion-fragment distributions produced in the electron-impact ionization of a neutral cluster. These experiments indicate that dimers contribute only to the ion signal H_3^+ , so that, for source conditions such that concentrations of trimers and larger clusters are negligible in comparison with the dimer concentration, the ion signal H_3^+ is a reliable measure of the dimer concentration. Hence the ratio of the mole fraction of the dimers, x_2 , to the monomers, x_1 , is calculated from

$$x_2/x_1 = I(6)/I(4)2\alpha \quad (1)$$

where $I(4)$ and $I(6)$ are the measured peak-area intensities at masses 4 and 6 amu, the factor of 2 accounts for the twice-as-large ionization probabilities of the dimers compared to the monomers, and the factor α corrects for the

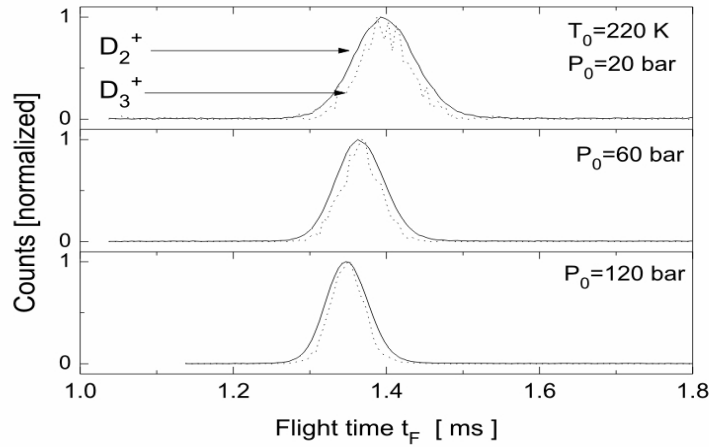


FIGURE 2. TOF spectra of the ion fragments D_2^+ (solid lines) and D_3^+ (dotted lines) for $T_0 = 220$ K and several values of P_0 . Source-orifice diameter is 10 μm . Flight distance is 2266 mm. Intensities are normalized.

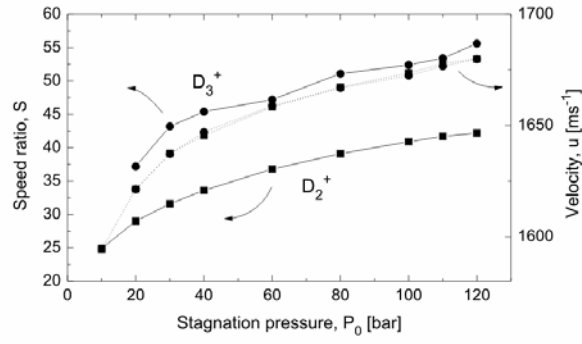


FIGURE 3. Pressure dependence of the speed ratios (solid lines) and terminal velocities (dotted lines) of the ion fragments D_2^+ and D_3^+ at $T_0 = 220$ K. Source-orifice diameter is $10 \mu\text{m}$.

effect of Mach-number focusing [32]. For this region, the relative concentration, x_2/x_1 , of rare-gas dimers has been shown [27,28] to be correlated as a function of the scaling parameter Γ which may be written

$$\Gamma = K_1^q K_2^{1-q} \quad (2)$$

where K_1 and K_2 are kinetic and thermodynamic parameters, respectively, defined by

$$K_1 = (P_0/kT_0)\sigma^3(d/\sigma)(\epsilon/kT_0)^{\gamma/(2\gamma-1)} \quad (3)$$

$$K_2 = (P_0/kT_0)\sigma^3(\epsilon/kT_0)^{1/(\gamma-1)} \quad (4)$$

Here k is the Boltzmann constant, σ is the zero-potential distance of the interaction potential, d is the source-orifice diameter, ϵ is the well depth of the interaction potential and γ is the specific-heat ratio of the monomers. The available data for terminal dimer concentrations in free-jet expansions of rare gases are correlated satisfactorily by $q = 0.4$ [27, 28].

In Fig. 4, the empirical fit obtained by Knuth from a detailed examination of terminal-dimer concentrations for Ar, Kr and Ne [27] is plotted as a dotted straight line. Values of the terminal D_2 -dimer mole fraction deduced from Eq. (1) also are shown as a function of the scaling parameter calculated with Eq. (2) and $q = 0.4$, $\sigma = 2.948 \text{ \AA}$, $\epsilon = 39.3 \text{ K}$ and $\gamma = 7/5$. In order to avoid significant contributions from ions originating from trimers and larger clusters, only data up to the cutoff pressures for which the value of the dimer mole fraction continues to increase approximately linearly with an increase in the value of the scaling parameter were included. It is seen that the terminal D_2 -dimer mole fractions measured for the pressure and temperature ranges investigated here are correlated to good

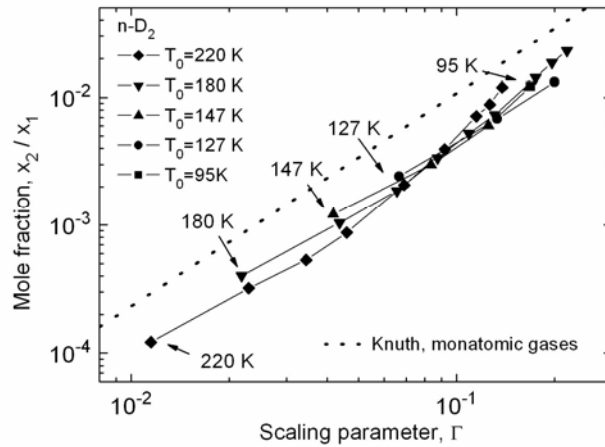


FIGURE 4. Mole fractions of D_2 as a function of the scaling parameter, Γ , defined in Eq. (2). The empirical fit for monatomic gases [27] is plotted as a straight dotted line.

approximation by a straight line drawn parallel to the correlating line established for the rare gases in Ref. [27]. For a given value of the scaling parameter, the dimer mole fraction for D_2 is about 40% of that for the rare gases. This deviation is ascribed to the increased random-translational temperature due to rotational relaxations, which was not taken into account in the scaling parameter. An analysis of the influence of rotational relaxation on dimer formation would require solving coupled equations of translational relaxation, rotational relaxation and dimer formation.

LARGE-CLUSTER FORMATION

Here the region in which large clusters dominate is examined. The recent matter-wave diffraction measurements of small neutral H_2 clusters [29] indicate that, for neutral clusters with more than about 37 molecules, the fragment-ion intensities for H_3^+ , H_5^+ and H_7^+ are nearly equal. This finding motivates an examination of the present measurements of fragment-ion intensities for neutral D_2 clusters – does a mass spectra with a uniform distribution of ion-fragment mass imply a neutral-clusters size equal to or larger than about 37 molecules?

The present measurements do indeed indicate that the fragment-ion intensities for D_3^+ , D_5^+ and D_7^+ approach nearly equal values as P_0 is increased for a fixed value of T_0 . See, e.g., Fig. 5. Hence, from similar sets of curves of ion-fragment intensity vs. P_0 for fixed T_0 , the value of the source pressure for which the D_3^+ intensity reaches its plateau was determined. For the range of source conditions investigated here, one obtains 120, 60, 40 and 20 bar, respectively, for $T_0 = 180, 147, 127$ and 95 K. If one uses now, as a first approximation, the correlation of cluster size with source conditions developed by Knuth [28] for the rare gases, then one obtains, for the lowest cluster sizes with nearly equal fragment-ion intensities, 40, 32, 32 and 40. These values are remarkably close to the value 37 found for H_2 . This agreement justifies the application of the cluster-size correlation for rare gases in order to predict D_2 cluster sizes for the source conditions investigated here. See Fig. 6.

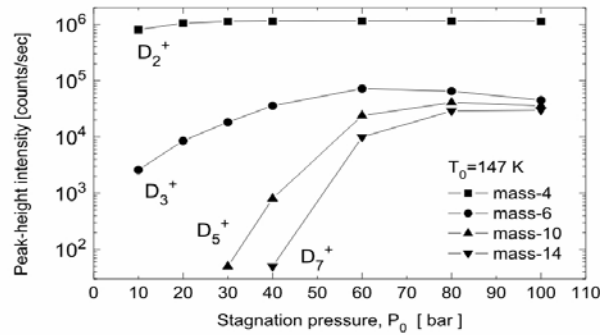


FIGURE 5. Intensities of the ion fragments D_2^+ , D_3^+ , D_5^+ and D_7^+ for $T_0 = 147$ K as functions of P_0 . Source-orifice diameter is $10 \mu\text{m}$.

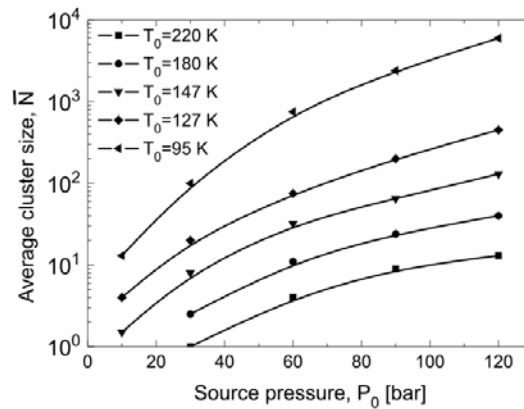


FIGURE 6. Estimated D_2 cluster size as function of source pressure for selected values of source temperature

CONCLUSIONS

The formation of D_2 clusters has been studied over a wide range of source temperatures (95-220 K) and source pressures (10-120 bar). The mass spectra reveal a predominance of odd-numbered cluster-ion fragments with magic values at D_9^+ and D_{15}^+ in agreement with previous work on H_2 cluster fragmentation. Much smaller signals, by one to two orders of magnitude, are observed for the even-numbered cluster-ion fragments. Distinct magic values were found at D_{10}^+ and D_{14}^+ .

The mass spectra indicate a substantially different behavior for the D_2^+ fragment ion compared with the larger fragment ions. This is interpreted as indicating that the D_2^+ signal is due largely to the unclustered molecules in the beam. In the dimerization regime the D_3^+ ion fragments are attributed to the dimers in the beam. This conclusion is supported by a scaling-parameter analysis which shows the same dimer-concentration trend as found for the rare gases. The reduction of the dimer mole fraction to 40% of the rare-gas value is attributed to the heating resulting from rotational relaxation.

The fragment-ion measurements indicate that their intensities approach nearly equal values as the source pressure is increased at a fixed source temperature – consistent with matter-wave diffraction measurements for H_2 clusters. A scaling-parameter analysis attributes this observation to a relatively flat fragment-ion distribution for D_2 clusters with more than about 36 molecules.

REFERENCES

1. W. Becker, K. Bier and W. Henkes, *Z. Phys.* **146**, 333-338 (1956).
2. A. van Deursen and J. Reuss, *Int. J. Mass Spect. And Ion Phys.* **11**, 483-489 (1973).
3. A. van Deursen, *Ph.D. Thesis*, Katholieke Universiteit te Toernooiveld, Nijmegen, The Netherlands, 1976.
4. A. van Deursen and J. Reuss, *Int. J. Mass Spect. and Ion Phys.* **23**, 109-206 (1977).
5. G. Tepper and D. Miller, *Phys. Rev. Lett.* **69**, 2927-2930 (1992).
6. G. Tejada, J.M. Fernandez, S. Montero, D. Blume and J.P. Toennies, *Phys. Rev. Lett.* **92**, 223401 (2004).
7. F. Buyvol-Kot, A. Kalinin, O. Kornilov, J.P. Toennies and J.A. Becker, *Solid State Comm.* **135**, 532-537 (2005).
8. E.W. Becker, R. Klingelhöfer and P. Lohse, *Z. Naturforschung* **17a**, 432-438 (1962).
9. K. Buchheit and W. Henkes, *Z. angew. Phys.* **24**, 191-196 (1968).
10. R. Klingelhöfer and H.O. Moser, *J. Appl. Phys.* **43**, 4575-4579 (1972).
11. E.L. Knuth, F. Schünemann and J.P. Toennies, *J. Chem. Phys.* **102**, 6258-6271 (1995).
12. B. Trostell, *Nucl. Instr. and Meth. in Phys. Res. A* **362**, 41-52 (1995).
13. A. Khokkaz, T. Lister, C. Quentmeier, R. Santo and C. Thomas, *Eur. Phys. J. D* **5**, 275-281 (1999).
14. J.E. Pollard, D.J. Trevor, J.E. Reutt, Y.T. Lee and D.A. Shirley, *J. Chem. Phys.* **77**, 34-46 (1982).
15. E.L. Knuth, S. Schaper and J.P. Toennies, *J. Chem. Phys.* **120**, 235-245 (2004).
16. J. Gspann and K. Korting, *J. Chem. Phys.* **59**, 4726-4734 (1973).
17. W. Obert, in *Rarefied Gas Dynamics*, edited by J.L. Potter, New York: AIAA, 1976, **2**, 1153-1162.
18. K. Kern, R. David and G. Comsa, *J. Chem. Phys.* **82**, 5673-5676 (1985).
19. D. Golomb, R.E. Good, A.B. Bailey, M.R. Busby and R. Dawbarn, *J. Chem. Phys.* **57**, 3844-3852 (1972).
20. R.M. Yealland, J.M. Decker, I.D. Scott and C.T. Tuori, *Can. J. Phys.* **50**, 2464-2470 (1972).
21. L.W. Bruch, W. Schöllkopf and J.P. Toennies, *J. Chem. Phys.* **117**, 1544-1566 (2002).
22. O.F. Hagena, *Surface Sci.* **106**, 101-116 (1981).
23. D. Golomb, R.E. Good and R.F. Brown, *J. Chem. Phys.* **52**, 1545-1551 (1970).
24. T.A. Milne, A.E. Vandergrift and F.T. Greene, *J. Chem. Phys.* **52**, 1552-1560 (1970).
25. O.F. Hagena and W. Obert, *J. Chem. Phys.* **56**, 1793-1802 (1972).
26. O.F. Hagena, *Z. Phys. D* **4**, 291-299 (1987).
27. E.L. Knuth, *J. Chem. Phys.* **66**, 3515-3525 (1977).
28. E.L. Knuth, *J. Chem. Phys.* **107**, 9125-9132 (1997).
29. J. Chaiken, J. Goodisman, A. Kalinin, O. Kornilov and J.P. Toennies, *J. Chem. Phys.*, in print.
30. Y. Ekinici and J.P. Toennies, *Phys. Rev. B* **72**, 205430 (2005).
31. D. Mathur and J.B. Hasted, *Nature (London)* **280**, 537-572 (1979).
32. P.K. Sharma, E.L. Knuth and W.S. Young, *J. Chem. Phys.* **64**, 4345-4351 (1976).